engineering proceedings

MDPI

Proceeding Paper

Histogram-Based Vehicle Black Smoke Identification in Fixed Monitoring Environments †

Meng-Syuan Tsai, Yun-Sin Lin and Jiun-Jian Liaw *

Department of Information and Communication Engineering, Chaoyang University of Technology, Taichung 41349, Taiwan; s11330621@gm.cyut.edu.tw (M.-S.T.); s11230608@gm.cyut.edu.tw (Y.-S.L.)

* Correspondence: jjliaw@cyut.edu.tw

† Presented at 8th International Conference on Knowledge Innovation and Invention 2025 (ICKII 2025), Fukuoka, Japan, 22–24 August 2025.

Abstract

The black smoke emitted by diesel vehicles poses a long-term threat to air quality and human health, with suspended particulate matter being the most significant concern. We developed an image-based black smoke detection system in this study. The system uses YOLOv9 to locate vehicles and vertically divides the bounding box into nine regions, selecting the bottom three as regions of interest. A reference baseline histogram is established from the first frame of the video under a non-smoke condition. For subsequent frames, a dynamic baseline histogram is calculated, and the presence of black smoke emissions is determined using baseline histogram differences. Experimental results confirm that the system can reliably identify black smoke-emitting vehicles in both dynamic and static environments.

Keywords: black smoke detection; image processing; histogram analysis; air pollution monitoring

1. Introduction

With increasingly congested urban traffic, diesel vehicle emissions have become one of the major sources of $PM_{2.5}$ pollution in Taiwanese cities, with an annual average contribution of up to 1.06 $\mu g/m^3$ [1]. This poses a serious threat to air quality and public health, as particulate matter penetrates the respiratory system, reaching the lungs and even entering the bloodstream. Long-term exposure increases the risk of cardiovascular diseases [2], respiratory illnesses [3], lung cancer [4], and strokes [5], posing a particularly serious threat to children, older adults, and individuals with chronic illnesses [6].

Traditional emission monitoring methods, such as visual inspection, monitoring stations, and periodic inspections, are limited by their lack of real-time capability, making it difficult to collect timely and frequent data. Recently, rapid developments and applications in image processing have made automatic black smoke detection a feasible direction. Researchers have proposed innovative image-based methods for detecting black smoke from vehicles. Spatial-depth video network [7] adopts a two-stage convolutional neural network, first detecting the characteristic regions of diesel vehicles and then performing fine-grained classification using a multi-region convolutional network. Enhanced small-target attention network [8] combines You Only Look Once (YOLO) v4 and a residual network, enhancing smoke detection performance through a spatial attention mechanism. To reduce interference from shadows, one study [9] utilized YOLOv5s in conjunction with superpixel segmentation and MobileNetv3 for image segmentation and classification. Another approach [10] introduced spatiotemporal feature learning by integrating Inception

check for updates

Academic Editors: Teen-Hang Meen, Chun-Yen Chang and Cheng-Fu Yang

Published: 3 February 2026

Citation: Tsai, M.-S.; Lin, Y.-S.; Liaw, J.-J. Histogram-Based Vehicle Black Smoke Identification in Fixed Monitoring Environments. *Eng. Proc.* **2025**, *120*, 24. https://doi.org/10.3390/engproc2025120024

Copyright: © 2026 by the authors. Licensee MDPI, Basel, Switzerland. This article is an open access article distributed under the terms and conditions of the Creative Commons Attribution (CC BY) license (https://creativecommons.org/licenses/by/4.0/).

V3, a multilayer perceptron, and long short-term memory to process image sequences and improve accuracy. Further methods include improving YOLOv5tiny with a smoke-vehicle matching strategy [11] or training models using black smoke datasets collected via on-board cameras [12]. Dual-branch network [13] employs a coarse-to-fine training strategy to improve regional prediction and recognition efficiency.

In traditional machine learning, R-Codebook integrates region-based visual local binary coding features [14] to enhance adaptability to environmental disturbances. S-BoF, combined with a pose-based convolutional neural network [15], extracts multiple image features and uses a support vector machine for classification. Another study [16] designed handcrafted features focused on vehicle tail characteristics, using a visual background extractor, gray-level co-occurrence matrix, and discrete wavelet transform for classification.

Overall, image-based black smoke detection techniques offer real-time performance and high accuracy, effectively addressing the limitations of traditional emission monitoring methods. We developed a black smoke detection system based on the baseline histogram difference (BHD) method. YOLOv9 was used to locate vehicles and then analyze the region behind the vehicle to compare pixel distribution differences between smoke and non-smoke conditions. A reference baseline histogram update mechanism (RBHUD) is also introduced to enhance environmental adaptability, ensuring robust smoke detection across varying lighting and recording conditions.

2. Black Smoke Vehicle Detection

2.1. Detection Method

The developed image-based system detects vehicles emitting black smoke. An overview of the detection process is shown in Figure 1.

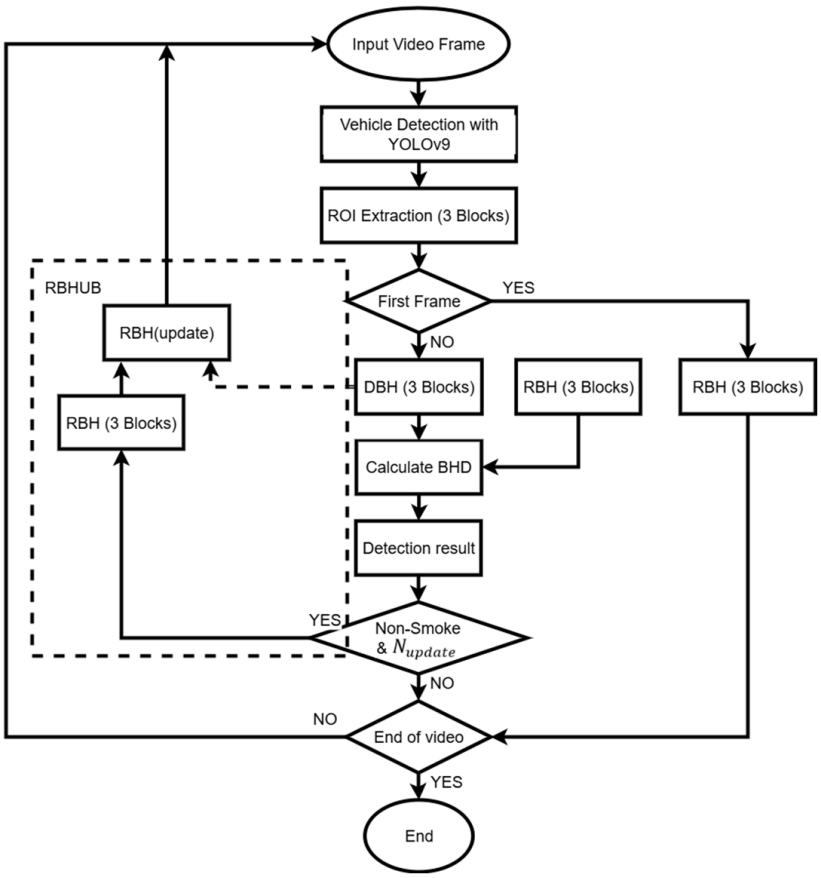


Figure 1. Black smoke vehicle detection process.

YOLOv9 is used to detect vehicles, and the bounding box is divided into nine vertical regions, with the bottom three designated as the region of interest (ROI). RBH is generated from the grayscale distribution of the first video frame. For each subsequent frame, a dynamic baseline histogram (DBH) is constructed, and the difference between RBH and DBH is measured using the BHD method to determine the presence of black smoke. To enhance adaptability to lighting variations, RBHUD is designed. RBH is updated only when a specific number of consecutive non-smoke frames are detected, to avoid incorrectly updating the baseline with frames containing black smoke. In addition, invalid frames are filtered based on aspect ratio and boundary position to eliminate recognition errors caused by turning vehicles or shifted camera angles.

2.2. Vehicle Detection

We adopted the YOLOv9–C model pretrained on the COCO dataset [13] for real–time vehicle detection. The programmable gradient information backbone and auxiliary reversible branch preserve salient features under lighting variation while maintaining inference speed.

2.3. ROI Definition

Because most exhaust pipes are located beneath the chassis, the bottom three strips of each vehicle's bounding box are treated as ROIs (Figure 2). This proportional partitioning naturally scales with distance and vehicle type, concentrating computation on the most probable smoke region and suppressing background clutter.



Figure 2. Illustration of ROI for black smoke detection. The green box indicates the detected vehicle bounding box, and the red boxes denote the ROI (the bottom three regions) used for subsequent histogram analysis.

2.4. Baseline Histogram Difference

By comparing the DBH of the current frame with the RBH under non-smoke conditions, the system determines whether black smoke emission is present. The comparison focuses

exclusively on low-gray-level bins (bin 1 and bin 2) to suppress background interference and non-smoke noise.

To quantify the difference in rear vehicle images between smoke and non-smoke states, this study proposes the Baseline Histogram (BH) as a feature representation. After converting the ROI to grayscale, pixel values are divided into eight bin intervals. The number of pixels in each bin is then counted to form a histogram, which is normalized to eliminate the effects of varying vehicle distances and sizes. The ROI in the first video frame is assumed to represent a non-smoke condition of the vehicle. Accordingly, a grayscale histogram is computed from the ROI of this frame and is defined as RBH. RBH is used to characterize the initial pixel distribution of the vehicle image and serves as the comparison basis for subsequent frames.

DBH is a histogram generated by performing grayscale pixel statistics on the rear ROI of the vehicle in each video frame. It represents the current pixel distribution of the image at that moment. The histogram of the current frame is first defined as $B_{i,j}^{DBH}$. By performing a bin-wise subtraction of the RBH from the DBH, the variation within each pixel range is obtained using Equation (1).

$$\Delta B_{i,j} = B_{i,j}^{DBH} - B_{i,j}^{RBH} \quad (1)$$

where $\Delta B_{i,j}$ represents the pixel variation within the given bin between the current image (DBH) and the non-smoke image (RBH). Here, $i \in \{1, 2, 3\}$ corresponds to the three ROI regions, and $j \in \{1, 2\}$ refers to bin 1 and bin 2. $B_{i,j}^{DBH}$ denotes the bin j value in ROI i of the current frame's DBH, while $B_{i,j}^{RBH}$ denotes the corresponding value in the RBH.

Black smoke emission is determined based on whether the variation in either bin exceeds a predefined threshold. If the variation $\Delta B_{i,1}$ in either bin 1 or bin 2 of ROI i exceeds a predefined threshold T, it is judged that black smoke emission has occurred in that ROI. The decision rule is defined as follows:

$$if\ \Delta B_{i,1} > T\ or\ \Delta B_{i,2} > T \quad . \quad (2)$$

To adapt to environmental changes, RBH is updated from DBH only when no black smoke is detected and the update interval (N_{update}) is reached. If black smoke is detected, the update is suspended to prevent contamination of the reference histogram. This update mechanism enhances the system's stability and ensures consistent long-term detection performance.

3. Result and Discussion

3.1. Datasets

The dataset used in this study comprised self-recorded video footage of vehicle exhaust emissions. A total of 2200 frames were extracted and manually annotated individually for each frame. The images were classified into two categories, black smoke and non-smoke, with 1100 frames allocated to each category to maintain class balance. The dataset was divided into training, validation, and testing sets based on their designated purposes. The detailed information of the dataset is shown in Table 1.

Table 1. The dataset used in this study.

Dataset	Black Smoke	Non-Smoke
Training	560	560
Validation	40	40
Testing	500	500
Total	1100	1100

3.2. Evaluation Metrics

To evaluate the accuracy and stability of the black smoke detection method, two metrics were adopted: accuracy and false alarm rate (FAR). These indicators provide a comprehensive assessment of the model's performance on both smoke and non-smoke samples. The formulas are defined as follows:

$$Accuracy = \frac{TP + TN}{TP + FN + FP + FN} \quad , \tag{3}$$

$$FAR = \frac{FP}{FP + TN} \quad , \tag{4}$$

where TP is the number of true positives (correctly detected smoke frames), TN is the number of true negatives (correctly detected non-smoke frames), FP is the number of false positives, and FN is the number of false negatives.

Both stationary and moving scenes were used to test the developed BHD method, and its performance was analyzed across different scenarios.

3.3. Result

To verify the accuracy and practicality of the proposed method, we compared the performance of the BHD method with a commonly used deep learning approach, ESA-Net, under identical testing conditions. The experimental parameters for the BHD method are set with a variation threshold $T > 15\%$ and an update interval of $N_{update} = 50$.

As shown in Table 2, the BHD method outperformed ESA-Net in both accuracy and FAR. The BHD method achieves an accuracy of 0.993, indicating near-perfect classification of black smoke and non-smoke images. Its FAR is 0.012, suggesting that only a small number of non-smoke frames were misclassified as smoke. In comparison, ESA-Net reaches an accuracy of 0.975, which is notably lower, and a slightly higher FAR of 0.014.

Table 2. Experimental results of black smoke identification.

Method	Accuracy	FAR
BHD	0.993	0.012
ESA-Net [8]	0.975	0.014

Detailed classification results are presented in Table 3. The BHD method outperforms ESA-Net in identifying both black smoke and non-smoke images. Among the 500 black smoke test frames, BHD successfully detected 499 TPs, with only 1 FN, whereas ESA-Net correctly identified 482. In terms of non-smoke classification, BHD also achieved slightly better performance, correctly classifying 494 TNs with only 6 FPs, while ESA-Net yielded 493 TNs and 7 FPs. Although the difference in negative class detection is small, BHD demonstrates more consistent and stable performance in non-smoke identification.

Table 3. Comparison of the confusion matrix.

Method	TP	FN	TN	FP
BHD	499	1	494	6
ESA-Net [8]	482	18	493	7

Figure 3 shows representative results of black smoke detection using the proposed BHD method. In each frame, the black smoke regions behind vehicles are accurately localized, illustrating the method's capability to capture pixel distribution changes associated with smoke emissions. These visual results are consistent with the quantitative

findings and further demonstrate the robustness and applicability of the proposed method in real-world scenarios.



(**a**) (**b**)

Figure 3. Black smoke detection results using the proposed BHD method: (**a**) detection of exhaust smoke near the tailpipe; (**b**) detection of dense black smoke emission. The red boxes indicate the ROI (the bottom three vertical regions of the detected bounding box) used for histogram analysis.

These results indicate that BHD achieves a more balanced classification performance. It consistently maintains high accuracy while effectively suppressing false detections. This advantage may be attributed to the histogram-based difference quantification mechanism employed by BHD, which enables the method to precisely capture subtle variations in low-gray-level pixels and thereby enhances its ability to identify black smoke characteristics.

4. Conclusions

We developed a black smoke vehicle detection method based on BHD, which effectively quantifies pixel-level changes, filters out non-smoke noise, and reduces false detection rates. In addition, the incorporation of the RBH update mechanism enhances the method's adaptability and stability under varying environmental conditions. The BHD method showed an accuracy of 0.993 and a FAR of 0.012, indicating excellent performance. The method developed offers high accuracy and strong potential for practical application. Further study is necessary to optimize the method for extreme lighting and dynamic environments to further improve its robustness.

Author Contributions: Conceptualization, J.-J.L. and Y.-S.L.; Methodology, Y.-S.L.; Software, Y.-S.L.; Validation, J.-J.L. and Y.-S.L.; Resources, M.-S.T. and Y.-S.L.; Supervision, J.-J.L.; Writing—Original Draft, M.-S.T. and Y.-S.L.; Writing—Review and Editing, M.-S.T. All authors have read and agreed to the published version of the manuscript.

Funding: This research received no funding support.

Institutional Review Board Statement: Not applicable.

Informed Consent Statement: Not applicable.

Data Availability Statement: The original contributions presented in this study are included in the article. Further inquiries can be directed to the corresponding author.

Conflicts of Interest: The authors declare no conflicts of interest.

References

1. Lu, H.-Y.; Wu, Y.-L.; Mutuku, J.K.; Chang, K.-H. Various sources of $PM_{2.5}$ and their impact on the air quality in Tainan City, Taiwan. *Aerosol Air Qual. Res.* **2019**, *19*, 601–619. [CrossRef]
2. Zhang, Q.; Meng, X.; Shi, S.; Kan, L.; Chen, R.; Kan, H. Overview of particulate air pollution and human health in China: Evidence, challenges, and opportunities. *Innovation* **2022**, *3*, 100312. [CrossRef] [PubMed]

3. Shahriyari, H.A.; Nikmanesh, Y.; Jalali, S.; Tahery, N.; Zhiani Fard, A.; Hatamzadeh, N.; Zarea, K.; Cheraghi, M.; Mohammadi, M.J. Air pollution and human health risks: Mechanisms and clinical manifestations of cardiovascular and respiratory diseases. *Toxin Rev.* **2022**, *41*, 606–617. [CrossRef]
4. Xue, Y.; Wang, L.; Zhang, Y.; Zhao, Y.; Liu, Y. Air pollution: A culprit of lung cancer. *J. Hazard. Mater.* **2022**, *434*, 128937. [CrossRef] [PubMed]
5. Kulick, E.R.; Kaufman, J.D.; Sack, C. Ambient air pollution and stroke: An updated review. *Stroke* **2023**, *54*, 882–893. [CrossRef] [PubMed]
6. Grigorieva, E.; Lukyanets, A. Combined effect of hot weather and outdoor air pollution on respiratory health: Literature review. *Atmosphere* **2021**, *12*, 790. [CrossRef]
7. Wang, X.; Kang, Y.; Cao, Y. SDV-net: A two-stage convolutional neural network for smoky diesel vehicle detection. In Proceedings of the 2019 Chinese Control Conference (CCC), Guangzhou, China, 27–30 July 2019; IEEE: Piscataway, NJ, USA, 2019; pp. 8611–8616.
8. Zhou, J.; Qian, S.; Yan, Z.; Zhao, J.; Wen, H. ESA-Net: A network with efficient spatial attention for smoky vehicle detection. In Proceedings of the 2021 IEEE International Instrumentation and Measurement Technology Conference (I2MTC), Glasgow, UK, 17–20 May 2021; IEEE: Piscataway, NJ, USA, 2021; pp. 1–6.
9. Wang, H.; Chen, K.; Li, Y. Automatic detection method for black smoke vehicles considering motion shadows. *Sensors* **2023**, *23*, 8281. [CrossRef] [PubMed]
10. Cao, Y.; Lu, X. Learning spatial temporal representation for smoke vehicle detection. *Multimed. Tools Appl.* **2019**, *78*, 27871–27889. [CrossRef]
11. Peng, X.; Fan, X.; Wu, Q.; Zhao, J.; Gao, P. Cascaded vehicle matching and short term spatial temporal network for smoky vehicle detection. *Appl. Sci.* **2023**, *13*, 4841. [CrossRef]
12. Yu, X.; Chang, X.; Chen, Q. Smoky vehicle detection based on YOLOv5 and car suppression. In Proceedings of the Third International Conference on Advanced Algorithms and Neural Networks (AANN 2023), Qingdao, China, 5–7 May 2023; SPIE: Bellingham, WA, USA, 2023; Volume 12791, pp. 555–559.
13. Chen, J.; Peng, X. DB Net: Detecting vehicle smoke with deep block networks. *Appl. Sci.* **2023**, *13*, 4941. [CrossRef]
14. Tao, H.; Lu, X. Smoke vehicle detection based on robust codebook model and robust volume local binary count patterns. *Image Vis. Comput.* **2019**, *86*, 17–27. [CrossRef]
15. Tao, H.; Lu, X. Smoke vehicle detection based on spatiotemporal bag of features and professional convolutional neural network. *IEEE Trans. Circuits Syst. Video Technol.* **2020**, *30*, 3301–3316. [CrossRef]
16. Tao, H.; Lu, X. Automatic smoky vehicle detection from traffic surveillance video based on vehicle rear detection and multi feature fusion. *IET Intell. Transp. Syst.* **2019**, *13*, 252–259. [CrossRef]

Disclaimer/Publisher's Note: The statements, opinions and data contained in all publications are solely those of the individual author(s) and contributor(s) and not of MDPI and/or the editor(s). MDPI and/or the editor(s) disclaim responsibility for any injury to people or property resulting from any ideas, methods, instructions or products referred to in the content.